PRAMANA
— journal of
physics

Vol. 73, No. 6
December 2009
pp. 999–1009

Synchronization and suppression of chaos in non-locally coupled map lattices

R M SZMOSKI[1], S E DE S PINTO[1], M T VAN KAN[2], A M BATISTA[2,*], R L VIANA[3] and S R LOPES[3]

[1]Departamento de Física; [2]Departamento de Matemática e Estatística, Universidade Estadual de Ponta Grossa, 84030-900, Ponta Grossa, PR, Brazil

[3]Departamento de Física, Universidade Federal do Paraná, 81531-990, Curitiba, PR, Brazil

[*]Corresponding author. E-mail: antoniomarcosbatista@gmail.com

MS received 23 February 2009; revised 12 June 2009; accepted 22 June 2009

Abstract. We considered coupled map lattices with long-range interactions to study the spatiotemporal behaviour of spatially extended dynamical systems. Coupled map lattices have been intensively investigated as models to understand many spatiotemporal phenomena observed in extended system, and consequently spatiotemporal chaos. We used the complex order parameter to quantify chaos synchronization for a one-dimensional chain of coupled logistic maps with a coupling strength which varies with the lattice in a power-law fashion. Depending on the range of the interactions, complete chaos synchronization and chaos suppression may be attained. Furthermore, we also calculated the Lyapunov dimension and the transversal distance to the synchronization manifold.

Keywords. Lattice; synchronization; maps; suppression.

PACS No. 05.45.Ra

1. Introduction

Lattice dynamical systems have been extensively studied as models of spatiotemporal complexity, due to the interplay between time and spatial degrees of freedom. Many phenomena observed in fluids and plasmas, like soliton propagation, travelling waves and turbulence are also present in lattice models, that are still able to retain some features of complex natural phenomena [1]. One of the most widely investigated type of spatially extended system is the coupled map lattice (CML), in which both space and time are discrete variables, but with a continuous state variable. A CML is basically composed of a local dynamical unit that undergoes discrete temporal evolution, interacting with other units through a given coupling prescription. Among the spatiotemporal features identified in coupled map lattices we can find synchronization of chaos [2], pattern formation [3], chaos suppression [4], intermittency [5–7] and multi-stability [8].

Most of the published work on CML have focussed on extreme cases of coupling, such as the local and global coupling. However, it is sometimes necessary to use forms of coupling which could include nonlocal interactions. One of the early studies focussing on the effects of nonlocal coupling is an investigation of coupled chaotic maps, with the range of coupling varying from local to global [9], where it was verified that the coupling takes on a global character well before the interactive term in the CML is mean field.

Here we focus on dynamical features such as synchronization and chaos suppression arising in an extended system where the interaction strength decays slowly with distance along the lattice in a power-law fashion. Such power-law coupling has been used in models of some biological neural networks [10]. It has also been considered in ferromagnetic spin models [11], self-organized memories in sliding charge density wave experiments [12] and in the synchronization transition of complex systems [13].

Other forms of nonlocal couplings that have seen considerable research interest involve a finite number of non-nearest neighbours, such as small-world networks. Such networks have been used to investigate the dynamics of coupled neural systems [14]. These have regular couplings with varying range, as well as some randomly chosen nonlocal interactions [15]. Also of interest are scale-free networks, where the connectivity is distributed according to a power law [16]. Lastly, random coupling, where all coupling connections are rewired randomly [17] has also been investigated.

Synchronization has been one of the collective phenomena most intensively studied, mainly after the discovery that chaotic systems, in spite of their natural instability, can synchronize their trajectories [18]. Such phenomena have applications in communications, heartbeat generation, neural activity [2,19], and coupled cells with activator–inhibitor pathways [20]. Synchronization results in a system as the outcome of the competition between two antagonistic factors: the intrinsic disorder caused by the nonlinear behaviour of each system unit and the diffusive effect provoked by their coupling [21]. It was observed in certain CMLs that the strictly nearest-neighbour coupling never allowed spatiotemporal synchronization, while synchronization arose with randomly rewiring connections [17,22]. So random (nonlocal) rewiring did enhance synchronization. This behaviour was also observed in networks of model neurons where the local dynamics had multiple time-scales such as spiking-bursting [19], as well as in networks of biochemical pathways [20].

The Lyapunov spectrum of a coupled map lattice gives us information about its degree of chaoticity, when one or more Lyapunov exponents are positive [23]. Many quantities of interest can be extracted from the Lyapunov spectrum of a coupled map lattice, like the maximal and mean Lyapunov exponents, the Kolmogorov–Sinai (KS) entropy, and the Lyapunov dimension. The KS entropy is particularly important since it is the asymptotic rate of creation of information by the dynamical system, and thus furnishes a quantitative measure of its degree of chaoticity. Moreover, the knowledge of the KS entropy enables us to apply the thermodynamical formalism, if the coupled map lattice model satisfies a large deviation statistics [24].

In this paper we will study a system with power-law coupling and focus on dynamical features such as complete synchronization and suppression of chaos. Therefore, this paper is organized as follows: in §2 we present the coupled map lattices with

long-range interaction. Section 3 presents the synchronization and suppression of chaos. Section 4 is devoted to analytical calculations of some particular cases of interest. The last section contains our conclusions.

2. Long-range coupled map lattices

Let x_n be a continuous dynamical state at discrete time $n = 0, 1, 2, \ldots$. A unidimensional lattice is formed with these maps, where the variable related to the ith site ($i = 1, 2, \ldots, N$) at time n is represented by $x_n^{(i)}$. Each unit has an evolution described by a map $x \mapsto f(x)$. We examine, in particular, a one-dimensional chain of N coupled logistic maps $x \mapsto rx(1-x)$, where $x_n^{(i)} \in [0, 1]$. The model to be treated is a modified version of the coupling in which the interaction strength between sites decays in a power-law fashion with the lattice distance

$$x_{n+1}^{(i)} = (1-\varepsilon) f(x_n^{(i)}) + \frac{\varepsilon}{\eta(\sigma)} \sum_{m=1}^{M} \frac{[f(x_n^{(i-j_m(q))}) + f(x_n^{(i+j_m(q))})]}{(j_m(q))^{\sigma}}, \qquad (1)$$

for $j_m(q) = q^m - 1$, resulting

$$x_{n+1}^{(i)} = (1-\varepsilon) f(x_n^{(i)}) + \frac{\varepsilon}{\eta(\sigma)} \sum_{m=1}^{M} \frac{[f(x_n^{(i-q^m+1)}) + f(x_n^{(i+q^m-1)})]}{(q^m-1)^{\sigma}}, \qquad (2)$$

where the interaction range is controlled by the exponent σ, ε is the coupling constant, and periodic boundary conditions are assumed. The sum in eq. (2) extends to $M = \log_q(N/2)$, and η is a normalization factor given by $\eta(\sigma) = 2\sum_{m=1,M}[j_m(q)]^{-\sigma}$.

Usually the model (eq. (1)) has been studied in the fully coupled case [4,13], i.e., for $j_m(q) = m$ with $M = (N-1)/2$. The coupling term is actually a weighted average of discretized spatial second derivatives, the normalization factor being the sum of the corresponding statical weights. Considering $j_m(q) = m$, the equation (1) reduces to the global mean-field in the limit $\alpha \to 0$, and when $\alpha \to \infty$ it reduces to the nearest-neighbour coupling. The coupling prescription (2) allows one to pass to a local Laplacian-type coupling when $\alpha \to \infty$, although this coupling does not reduce to the global mean-field when $\alpha \to 0$. Tessone and coworkers [25] have shown that two coupled replicas of such systems (eq. (2)) synchronize to a common spatiotemporal chaotic state above a certain coupling strength.

3. Synchronization and suppressions of chaos

A completely synchronized state takes place when the dynamical variables which define the state of each map adopt, after a transient, the same value for all the coupled maps at all times n, i.e., $x_n^{(1)} = x_n^{(2)} = \cdots = x_n^{(N)} \equiv x_n^{(*)}$. It can be easily verified that this state is the solution of eq. (2). Depending on the number of maps and the range of the interactions, there may exist an interval of values of the

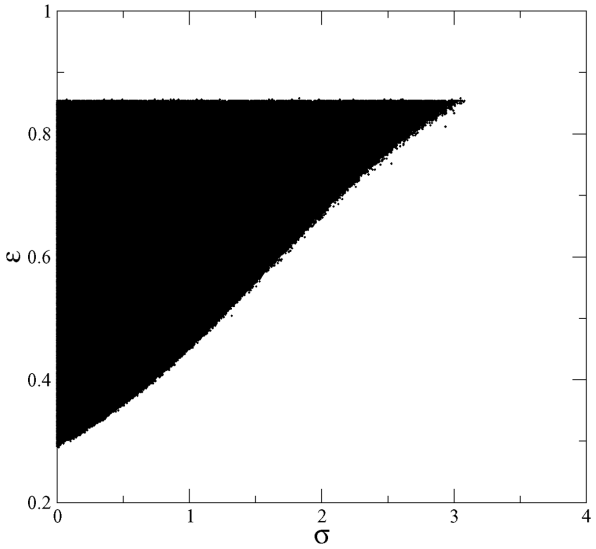

Figure 1. Synchronization domains (black region) in parameter plane $\varepsilon \times \sigma$ with $r = 3.69$ and $N = 8$.

coupling strength ε, for which such a state is spontaneously attained, as we have analytically shown in a previous work [26].

A numerical diagnosis of chaos synchronization is provided by the order parameter $z_n = R_n \exp(2\pi i \varphi_n) \equiv (1/N) \sum_{j=1}^{N} \exp(2\pi i x_n^{(j)})$, where R_n and φ_n are the amplitude and angle, respectively, of a centroid phase vector, for a one-dimensional chain with periodic boundary condition [27]. A time-averaged amplitude $R_m = \lim_{T\to\infty}(1/T) \sum_{n=0}^{T} R_n$ is computed over an interval large enough to warrant that the asymptotic state has been achieved by the lattice. A chaos synchronization state implies $R_m = 1$, for all the phase vectors gyrate together with the same phase. When the maps are completely nonsynchronized, on the other hand, we get a pattern in which the site amplitudes $x_n^{(j)}$ are so spatially uncorrelated that they may be considered essentially as random variables, such that R_m vanishes. We investigate the dependence of the average order parameter magnitude R_m on the quantities characterizing coupling (strength vs. effective range). Figure 1 shows this dependence, where we separate regions with: (i) synchronized chaotic orbits (black region) and (ii) nonsynchronized orbits (white region).

The synchronization region depends on the lattice size. Figure 2 shows the horizontal length of synchronization region $\sigma_{\max}$ for $\varepsilon = 0.85$ and $N = 8$, 16, 32, 64, 128, 256, 512, 1024. We observe that $\sigma_{\max}$ obeys a power-law scaling with the lattice size.

We also computed the Lyapunov spectrum of the coupled map lattice to obtain another quantity of interest, that is, the Lyapunov dimension. The corresponding Lyapunov spectrum of a lattice with N coupled one-dimensional maps is formed by N exponents, one for each independent eigendirection in the tangent space: $\lambda_1 = \lambda_{\max} > \lambda_2 > \cdots > \lambda_N$. The exponents are obtained as $\lambda^{(k)} = \ln \Lambda^{(k)}$, for

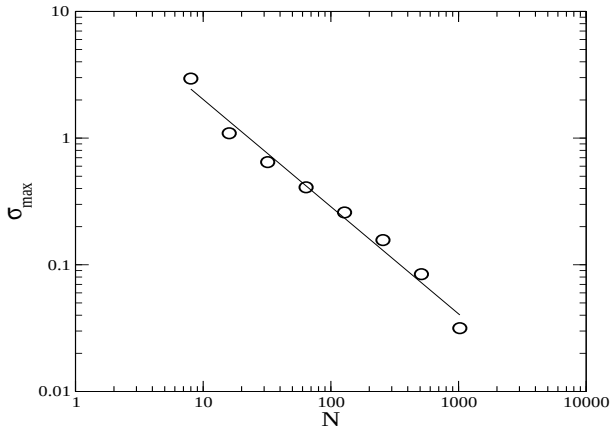

Figure 2. Horizontal length of synchronization region vs. lattice size with $\sigma_{\max} = \alpha N^{\beta}$, where $\alpha = 14.595$ and $\beta = -0.851$.

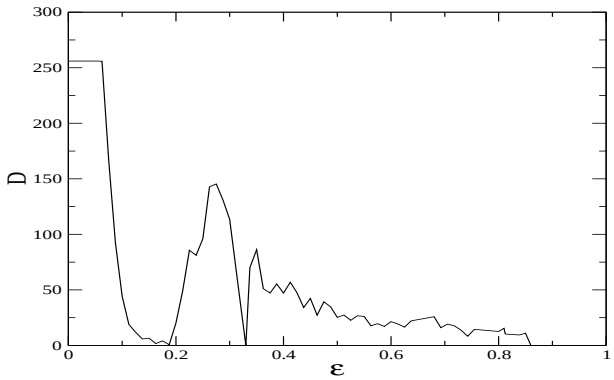

Figure 3. Lyapunov dimension of the coupled map lattice vs. coupling strength, for $r = 3.69$, $\sigma = 0$ and $N = 256$.

$k = 1, \ldots, N$, where $\Lambda^{(k)}$ are the eigenvalues of the product of n Jacobian matrices.

Let p be the greatest integer for which $\sum_{j=1}^{p} \lambda_j$ is positive. The Lyapunov dimension is defined as [28]

$$D = \begin{cases} 0 & \text{if there is no such } p \\ p + \frac{1}{|\lambda_{p+1}|} \sum_{i=j}^{p} \lambda_j & \text{if } p < N \\ N & \text{if } p = N \end{cases} . \tag{3}$$

Thus, if the system presents suppression of chaos we have $D = 0$.

We identify, in figure 3, chaos suppression for $\varepsilon = 0.16$ and 0.33. The interval $0.70 < \varepsilon < 0.85$ characterizes synchronization of chaos. For $\varepsilon > 0.85$ the lattice exhibits chaos suppression and quasiperiodicity.

Since N is usually a large integer, a direct approach to the transversal dynamics is extremely difficult unless we appeal to some kind of approximation to reduce the number of degrees of freedom involved, such as computation of the transversal

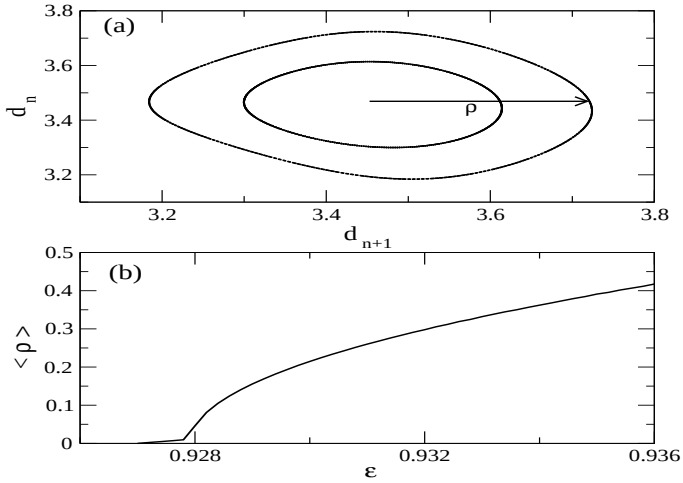

Figure 4. (**a**) First return plot for d, with $r = 3.69$, $\sigma = 0.0$, $\varepsilon = 0.929$ (minor circle) and $\varepsilon = 0.931$ (large circle) and (**b**) mean radius $\langle\rho\rangle$ vs. ε.

distance to the synchronization manifold, $d_n = \mu_n\sqrt{N}$, where μ_n is the standard deviation of the state variable values around their spatially averaged value at time n [4]. Thus $d = 0$ for a completely synchronized state. Near the parameter value 0.928, where $D = 0$ (figure 3), we observe chaos suppression, but this time yielding a quasiperiodic orbit, i.e., the map iterations densely fill an invariant curve that is the section of a high-dimensional torus. The emergence of such an invariant curve from a fixed point occurs due to a Neimerk–Sacker bifurcation at the critical value of the coupling parameter. This quasiperiodic orbit breaks up, yielding a chaotic attractor whose dimension increases with ε, except for tiny periodic windows in the bifurcation diagram. Some of these orbits are shown in figure 4a, where we calculate the first return map of d for two values of ε, yielding invariant curves or two-bidimensional sections of a high-dimensional torus outside the synchronization manifold. These curves are topological circles with radius $\rho(d_n)$ and centred at $d = 3.45$, which is the stable fixed point existing just before a Neimark–Sacker bifurcation. Just after the bifurcation the radius of the invariant circle increases as $\rho \sim |\varepsilon - 0.928|^{1/2}$ [29], which agrees with the mean radii $\langle\rho\rangle$ of the invariant curves we have numerically determined (figure 4b).

In figure 5a, we depict the transversal distance to the synchronization manifold d vs. control parameter r, for $N = 256$. We can observe a small length Δr of chaos suppression for $r > 3.98$, which varies with the parameter σ. We verified that Δr depends on σ, diminishing linearly when we increase the range parameter (figure 5b).

4. Analytical results for the Lyapunov spectrum and KS entropy

The Lyapunov spectrum is obtained from the dynamics of tangent vectors ξ, which in turn is obtained by differentiation of the original evolution equations. In matrix

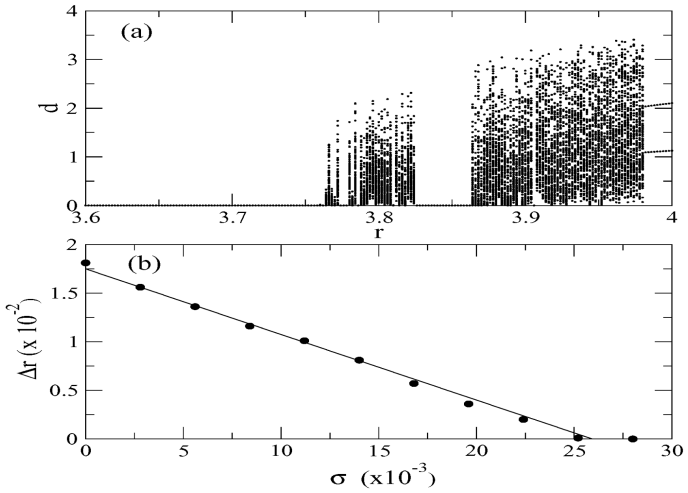

Figure 5. (**a**) d vs. r for $\varepsilon = 0.75$ and $\sigma = 0$, (**b**) Δr vs. σ for $\varepsilon = 0.75$ with $\Delta r = -0.067\sigma + 1.749$.

form the tangent dynamics reads $\xi_n = \Gamma_n \xi_0$, where Γ_n is a product of n Jacobian matrices calculated at successive points of a given trajectory. If $\Lambda^{(1)}, \ldots, \Lambda^{(N)}$ are the eigenvalues of $\lim_{n\to\infty}(\Gamma_n^T \Gamma_n)^{1/2n}$, the Lyapunov exponents are obtained as $\lambda^{(k)} = \ln \Lambda^{(k)}$, for $k = 1, \ldots, N$. Evaluating the Jacobian matrices along the synchronized trajectories, one arrives at the following expression for the Lyapunov spectrum [26]:

$$\lambda_k = \lambda_u + \ln\left|1 - \varepsilon + \frac{\varepsilon}{\eta(\sigma)} b^{(k)}\right|, \tag{4}$$

where $\lambda_u > 0$ is the Lyapunov exponent of the uncoupled chaotic map and $b^{(k)}$ are the eigenvalues that can be obtained by Fourier diagonalization and read

$$b^{(k)} = 2 \sum_{m=1}^{M} \frac{1}{(q^m - 1)^\sigma} \cos\left[\frac{\pi k (q^m - 1)}{q^M}\right]. \tag{5}$$

The maximal Lyapunov exponent is λ_u, and it typically varies with k and the Lyapunov spectrum may assume qualitatively different features according to the values assumed by the coupling strength and range parameter, which is schematically shown in figure 6 for some exponents. We observe in figures 6a and 6b that the value of k of the second largest Lyapunov exponent can depend on σ for fixed ε.

The chaos synchronization state will be transversely stable if the $(N-1)$ remaining exponents are negative, that is, $|1-\varepsilon+\varepsilon b^{(k)}/\eta| < \mathrm{e}^{-\lambda_u}$. This is equivalent to the requirement that the second largest (or largest transversal) asymptotic exponent, denoted by $\lambda^\perp$, be negative. The condition $\lambda^\perp < 0$ leads to $\varepsilon_c < \varepsilon < \varepsilon_c'$, where

$$\varepsilon_c = (1 - \mathrm{e}^{-\lambda_u}) \left[1 - \frac{1}{\eta(\sigma)} b^{(j)}\right]^{-1}, \tag{6}$$

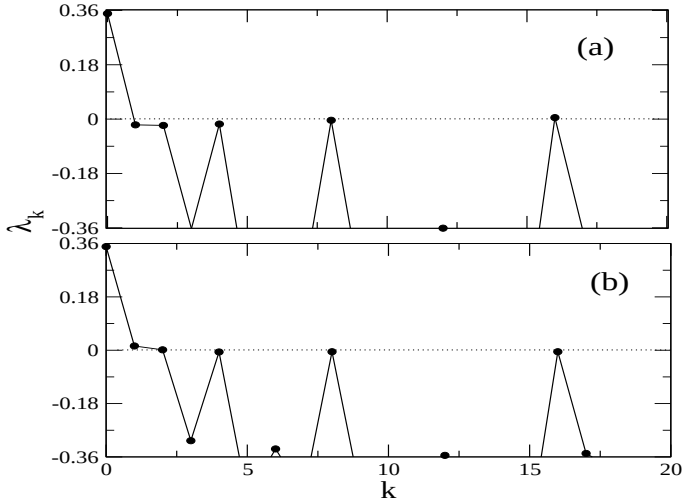

Figure 6. Lyapunov spectrum with $r = 3.69$, $q = 2$, $M = 7$, $\varepsilon = 0.68$, (**a**) $\sigma = 0.03$ and (**b**) $\sigma = 0.07$.

$$\varepsilon_c' = (1 + \mathrm{e}^{-\lambda_u}) \left[1 - \frac{1}{\eta(\sigma)} b^{(q^M)} \right]^{-1}, \tag{7}$$

where j is the value of k that is obtained for $\lambda_k = \lambda^{\perp}$ in eq. (4). For example, considering $M = 7$ we have $j = 16$ for $\sigma < 0.05$ and $j = 1$ for $\sigma > 0.05$ (figure 6).

In figure 7 we show a variety of critical curves in parameter space (α, ε) obtained for different M. The critical curves were obtained analytically from eqs (6) (lower curve) and (7) (upper curve). The symbols shown stand for the numerical results determined from the condition $R_m = 1$ with a tolerance of 10^{-6}.

For coupled chaotic maps many exponents are positive, hence a quantity of interest is the average sum of the positive Lyapunov exponents

$$h = \langle \lambda_k \rangle_{k,\lambda_k>0} = \frac{1}{N} \sum_{k=1}^{\lambda_k>0} \lambda_k. \tag{8}$$

If the dynamical system is a diffeomorphism with an invariant ergodic measure absolutely continuous with respect to the Lebesgue measure, then this quantity is equal to the density of KS entropy, which is the symptotic rate of creation of information by successive iterations of the dynamical process (Pesin's theorem) [30]. For C^1 maps preserving an ergodic measure, h is an upper bound for the KS entropy. The equality between h and the density of KS entropy is generally valid for systems having a Sinai–Ruelle–Bown (SRB) measure, like Axiom-A systems [31].

Substituting Lyapunov spectrum (4) into (8) gives KS entropy in terms of a summation which, generally, does not have a closed analytical form. Appproximate values, however, can be obtained by supposing that the lattice is so tightly packed that the distance between sites k is small enough to allow us to consider it as a continuous value, and to replace the summation by an integral

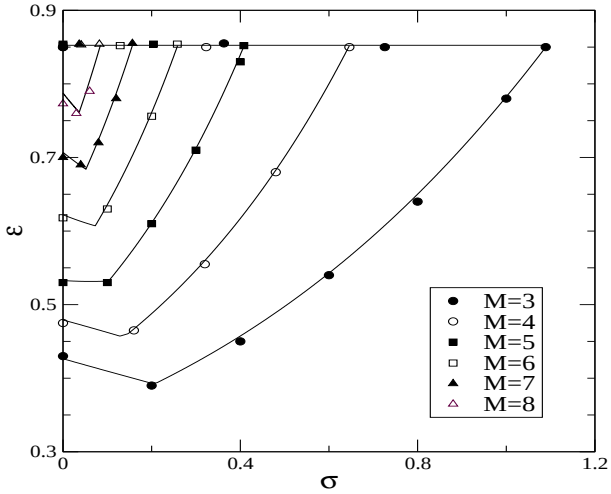

Figure 7. Synchronization diagram in parameter space (α, ε), for different values of M. Lines correspond to analytical predictions and symbols to numerical simulations.

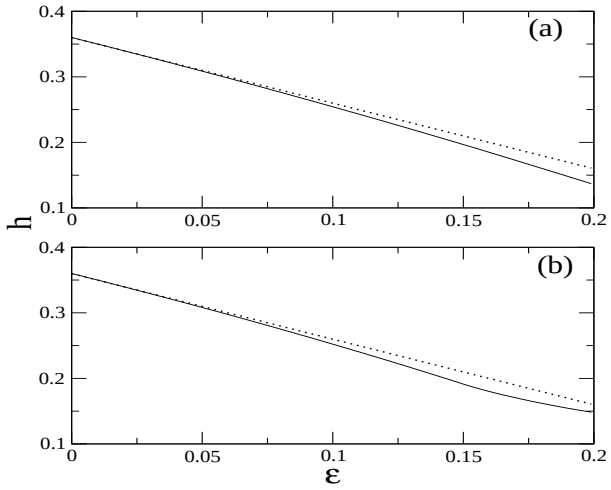

Figure 8. KS entropy density vs. coupling strength. The analytical results from eq. (10) are shown with dotted line and solid line represents the numerical result. We considered $r = 3.69$, $q = 2$, $M = 10$, (**a**) $\sigma = 0.0$ and (**b**) $\sigma = 2.0$.

$$h(\varepsilon) = \frac{1}{N} \int_{\lambda>0} \lambda_k \mathrm{d}k. \tag{9}$$

We can obtain an approximate analytical value for the integral for the case of small coupling as well as Lyapunov spectrum with all positive exponents. Defining $y = -\varepsilon + \varepsilon b^{(k)}/\eta(\sigma)$ enables us to expand the integrand in powers of y $(-1 < y < 1)$ so that $\ln(1+y) = y - y^2/2 + \cdots$. Considering first-order term we have the result

$$h(\varepsilon) = \frac{(N-1)(\lambda_u - \varepsilon)}{N} + \frac{2\varepsilon q^M}{N\pi\eta(\sigma)} \sum_{m=1}^{M} \frac{1}{(q^m-1)^{\sigma+1}} \times \left\{ \sin\left[\frac{\pi N(q^m-1)}{q^M}\right] - \sin\left[\frac{\pi(q^m-1)}{q^M}\right] \right\}. \quad (10)$$

In figure 8 we compare the (exact) numerical result for the KS entropy density with the appproximation obtained from eq. (10) by retaining first-order term. We see that the agreement between numerical and analytical results is very good for $\varepsilon < 0.1$.

5. Conclusions

In this paper we studied some aspects of the spatiotemporal dynamics displayed by a coupled map lattice with long-range interactions. Our numerical results indicated that the synchronization region decreases when the lattice increases. We observed suppression chaos and quasiperiodicity by means of the Lyapunov dimension and the transversal distance. We verified another instance of chaos suppression, but this time yielding a quasiperiodic orbit, i.e., the map iterations densely fill an invariant curve which is the section of a high-dimensional torus. We have presented analytical expressions for the Lyapunov spectrum of coupled map lattice with interaction which decays with the lattice distance as a power-law. Our results enable us to predict the critical values for synchronization in the coupling parameter plane, and also we obtained related quantities of interest, such as KS entropy. For weak coupling the entropy density decreases from its maximum value, that is in agreement with numerical results.

Acknowledgements

This work was made possible by partial financial support from the following Brazilian government agencies: CNPq, CAPES and Fundação Araucária (Paraná).

References

[1] J P Crutchfield and K Kaneko, in: *Directions in chaos* edited by Hao Bain-Lin (World Scientific, Singapore, 1987) Vol. 1, p. 272
[2] A Pikovsky, M Rosemblum and J Kurths, *Synchronization: A universal concept in nonlinear sciences* (Cambridge University Press, Cambridge, England, 2001)
[3] T Shibata and K Kaneko, *Physica* **D181**, 197 (2003)
P G Lind, J Corte-Real and J A C Gallas, *Phys. Rev.* **E69**, 066206 (2004)
[4] S E de S Pinto, I L Caldas, A M Batista, S R Lopes and R L Viana, *Phys. Rev.* **E76**, 017202:1-4 (2007)
[5] R L Viana, C Grebogi, S E de S Pinto, S R Lopes, A M Batista and J Kurths, *Physica* **D206**, 94 (2005)
[6] Z Jabeen and N Gupte, *Phys. Rev.* **E74**, 016210 (2006)

[7] Z Jabeen and N Gupte, *Pramana – J. Phys.* **70(6)**, 1055 (2008)
[8] A Lemmaitre and H Chaté, *Phys. Rev. Lett.* **82**, 1140 (1999)
[9] S Sinha, D Biswas, M Azam and S V Lawande, *Phys. Rev.* **A46(10)**, 6242 (1992)
[10] J C A de Pontes, R L Viana, S R Lopes, C A S Batista and A M Batista, *Physica* **A387**, 4417 (2008)
[11] S A Cannas and F A Tamarit, *Phys. Rev.* **B54**, R12661 (1996)
[12] J C A de Pontes, A M Batista, R L Viana and S R Lopes, *Physica* **A368**, 387 (2006)
[13] R L Viana, C Grebogi, S E de S Pinto, S R Lopes, A M Batista and J Kurths, *Phys. Rev.* **E68**, 067204 (2003)
[14] P M Gade and S Sinha, *Int. J. Bifurcat. Chaos* **16(9)**, 2767 (2006)
[15] A M Batista, S E de S Pinto, R L Viana and S R Lopes, *Physica* **A322**, 118 (2003)
[16] C A S Batista, A M Batista, J A C de Pontes, R L Viana and S R Lopes, *Phys. Rev.* **E76**, 016218:1-10 (2007)
[17] S Sinha, *Phys. Rev.* **E66**, 016209 (2002)
[18] L M Pecora and T L Carroll, *Phys. Rev. Lett.* **64**, 821 (1990)
[19] M P K Jampa, A R Sonawane, P M Gade and S Sinha, *Phys. Rev.* **E75**, 026215 (2007)
[20] S Rajesh, S Sinha and S Sinha, *Phys. Rev.* **E75**, 011906 (2007)
[21] S Bocalletti, J Kurths, G Osipov, D L Valladares and C S Zhou, *Phys. Rep.* **366**, 1 (2002)
[22] A Mondal, S Sinha and J Kurths, *Phys. Rev.* **E78**, 066209 (2008)
[23] A M Batista and R L Viana, *Phys. Lett.* **A286**, 134 (2001)
[24] H Shibata, *Physica* **A292**, 182 (2001)
[25] C J Tessone, M Cecini and A Torcini, *Phys. Rev. Lett.* **97**, 224101 (2006)
[26] C Anteneodo, S E de S Pinto, A M Batista and R L Viana, *Phys. Rev.* **E68**, 045202(R) (2003)
C Anteneodo, A M Batista and R L Viana *Phys. Lett.* **A326(3–4)**, 227 (2004)
[27] S E de S Pinto and R L Viana, *Phys. Rev.* **E61**, 5154 (2000)
[28] E Ott, *Chaos in dynamical systems* 2nd ed. (Cambridge University Press, Cambridge, UK, 2002)
J-P Eckmann and D Ruelle, *Rev. Mod. Phys.* **57**, 617 (1985)
[29] S Wiggins, *Introduction to applied nonlinear dynamical systems and chaos* (Springer-Verlag, New York, 1990)
[30] Y B Pesin, *Russ. Math. Surv.* **32**, 55 (1977)
[31] D Ruelle, *Chaotic evolution and strange attractors* (Cambridge University Press, Cambridge, 1989)